GMR
The Original

CANCER METASTASES IN THE BRAIN BASED ON FUZZY GENETIC ALGORITHM AND ARTIFICIAL NEURAL NETWORK

Jeyavani M[1], Vidhya Saraswathi P[2]

[1]Department of Computer Applications, Kalasalingam Academy of Research and Education, Krishnankoil, Tamil Nadu – 626126, 0000-0002-0929-1532
[2]Department of Computer Science & Information Technology, Kalasalingam Academy of Research and Education, Krishnankoil, Tamil Nadu – 626126, 0000-0002-3188-3489

ABSTRACT

Cancer cells can metastasize to the brain when they move from their primary site. The symptoms of metastases are influenced by the location, size, and number of growths within the brain as well as the degree of swelling. The growing metastatic brain tumors are putting pressure on the nearby brain tissue. Therefore, among the common symptoms are headaches, the inability to move an arm or a leg, sleepiness, memory loss, personality changes, seizures, and nausea or vomiting, most frequently happening. After the age of 45, the risk of developing a metastatic brain tumor rises, reaching its peak in people over the age of 65. The newly proposed method is to extract the two various metastasised lung and melanoma cancers from brain metastases. The most dangerous cancer is lung cancer which develops from the lung tissue, and the most dangerous type of skin cancer is melanoma which can appear anywhere on the body. Hence, currently, a novel system for MRI is utilized to find the rapid growth of brain metastases cancer cells in aberrant tissue that is lung cancer (LC) or Melanoma Cancer (MC). Hence a hybrid technique for automatic lung cancer brain metastases (LCBM) and Melanoma Cancer brain metastases (MCBM) detection using simultaneous feature selection with a Fuzzy Genetic Algorithm (FGA) and Artificial Neural Network (ANN) is proposed here to show the classification performance analysis to solve regression problems. The suggested technique uses Rtool and an MRI clinical dataset to identify the affected region of brain cancer metastases.

GRAPHICAL ABSTRACT

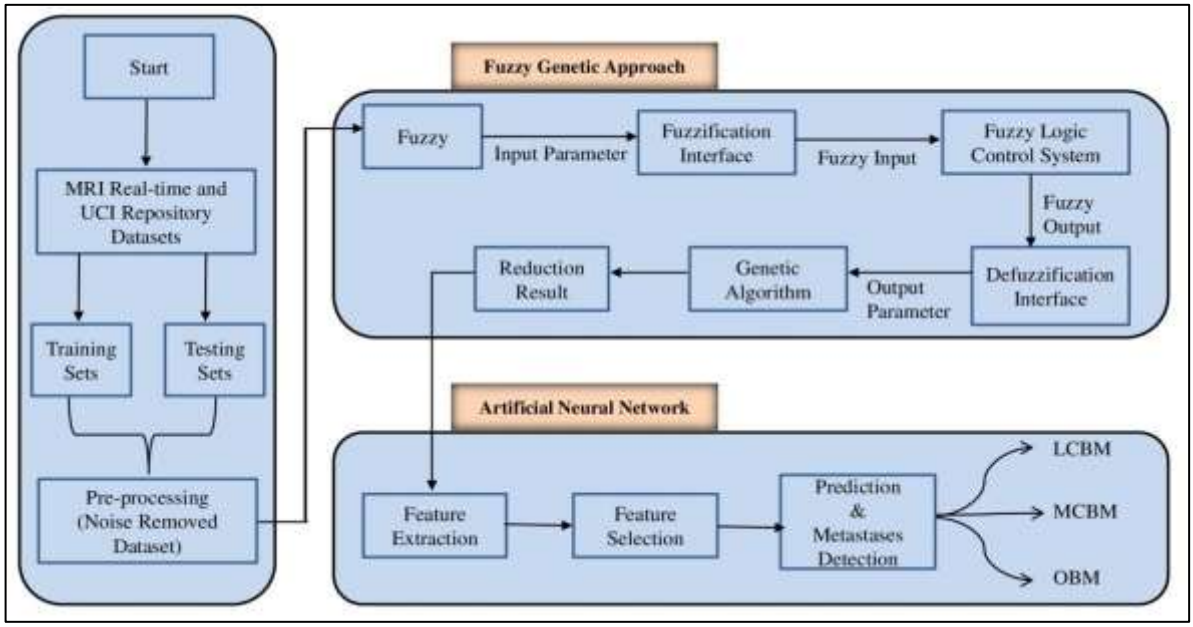

Figure 1. Prediction of Cancer Metastases in the Brain using FGA-ANN

KEYWORDS*:* Fuzzy Genetic Algorithm (GA), Artificial Neural Network (ANN), Lung Cancer Brain Metastases (LCBM), Melanoma Cancer Brain Metastases (MCBM), Magnetic Resonance Imaging (MRI), Good Health and Well-Being.

1. INTRODUCTION

Lung, Breast, Colon, and Kidney cancers. Brain metastases have led to the development of one or more tumors. Metastatic Cancer cells can spread to the brain when they leave their brain tumors put pressure on the nearby brain tissue as they original site, and form metastases in the brain. Any cancer can grow. Brain metastasis may result in the growth of one or more brain tumors. Breast, Melanoma, and Lung Cancer patients are more likely than those with other cancer types to experience Brain Metastases. With the help of this technique, Brain Metastases as well as underlying cancers like lung cancer, melanoma, and other cancer types have been discovered simultaneously. Even though isolated areas of Brain

Metastases are common, meningitis has been caused by some cancer types (swelling of the linings of the brain). Lymphomas, leukaemias, and extremely advanced forms of other the most prevalent types of cancer are cancers where this occurs. Differentiating between meningitis and cancer-related symptoms can be more difficult. Dexamethasone, a topical steroid medication, is used to lessen swelling around Brain Metastases. While additional treatment is being planned, this frequently helps to immediately relieve symptoms.

The most dangerous type of brain tumor is brain metastasis, which is a serious side effect of cancer, anywhere between 10% and 26% of cancer patients who pass away experience Brain Metastases [1]. Every year, 170,000 patients in the US are diagnosed with brain metastases, accounting for about one-fourth of all cancer metastases. The proportion of patients presenting with brain metastasis is rising as molecularly targeted therapies, immunotherapies, and improvements in stereotactic radiation therapy increase the chances of survival for cancer patients. After receiving treatment, many patients with brain metastases do not experience the long-term cognitive impairment brought on by whole-brain radiation. Although the increased chance of survival is a significant advancement in cancer treatment, it also highlights the need for exact follow-up and the timely identification of brain metastases. Stereotactic radiosurgery (SRS) and stereotactic radiotherapy (SRT) are very effective treatments when brain metastases are found early and are small. For instance, SRT can be used to treat additional or fresh metastases at various times without going over the critical radiation dose thresholds. Because of these developments, radiologists must find all metastases during every subsequent brain magnetic resonance imaging (MRI) scan, which can contain more than 150 slices in a single scan. Radiologists are frequently asked today to monitor 20 or more metastases that have received SRS at various times over the years. Many metastases exhibit a decrease in size and post-contrast prominence following treatment. The only available treatments after that point were whole-brain radiation and hospice care, so monitoring more than three or four Brain Metastases was uncommon ten years ago. Brain MRI interpretation is now a much more important, difficult, and time-consuming task. Small size, similarity to small blood vessels, and low contrast-to-background ratio (CBR) on the brain dataset are the main barriers to metastasis detection. Radiologists must scroll back and forth through adjacent slices to distinguish a metastasis from the surrounding vessels, which is a time-consuming and error-prone process even though small metastases are frequently only visible on a single MRI slice. Because it is unknown whether or how many metastases are present in specific brain MRI sections before detection, this search task is made more difficult.

Brain Metastases increase cancer patients' morbidity and mortality, according to the National Center for Biotechnology Information. About 25% of all cancer patients have them, which is a ratio of 10:1 more than primary brain tumors. Conservative estimates indicate that there are 100,000–170,000 new cases of brain metastases in the United States each year. Brain metastases are discovered in 20% to 40% of patients with metastatic cancer who undergo autopsies. Most patients with brain metastases have primary cancer, which is well-known. Lung (40-50%), breast (15-25%), melanoma (5-20%), and kidney (5-10%) cancers are the most common sites for brain metastases. 80% of patients who have brain metastases do so in the cerebral hemispheres, 15% do so in the cerebellum, and 5% do so in the brainstem.

This study investigated whether texture analysis (TA) of T1 post-contrast MRI datasets could be used to distinguish between different types of Lung and Melanoma Cancers in the Brain Metastases. Due to rising lung cancer and melanoma rates, more sensitive detection methods, and improvements in anticancer treatment that have increased survival time, there appears to be an increase in brain secondary cases in recent years. Non-Small Cell Lung Cancer (NSCLC) patients are 30-43 % more likely to develop BM on their own, without any other signs of metastatic disease, and 30-54 % more likely to do so after treatment. Patients with NSCLC BM have an average survival time of 7-8 months [3]. Additionally, BM is predicted to have a poor prognosis and few curative options. Gender has no bearing on the overall incidence of Brain Metastases, but males are more likely than females to have melanoma spread to the brain. The effect of the current research indicated that the male and female sexes are distributed almost equally (52.78% vs. 47.22%). Stage IV melanoma has metastasized (spread) to other parts of the body during these four stages, including the brain, lungs, liver, and gastrointestinal (GI) tract. Studies show that between 40% and 75% of melanoma patients will develop one or more brain metastases. The 5-year mortality rate for melanoma ranges from 97% (stage IA disease) to 40%. (stage IIIC). The 5-year survivability rate for metastatic melanoma is about 15% [2].

The most frequent causes of Brain Metastases are used in our new methodology to demonstrate how we categorize the performance for the early detection of LCBM and MCBM. Advances in neuroradiology have had a significant positive impact on the diagnosis and treatment of patients with suspected neoplastic diseases of the central nervous system (CNS). The widespread use of contrast-enhanced computed tomography (CECT) is a result of its affordability and ease of use. Contrastenhanced magnetic resonance imaging (MRI) is more sensitive than enhanced computed tomography (CT) scanning to identify small lesions or brain metastases. To reduce mortality rates and treatment costs, MRI was used as a new technique for the early diagnosis of Brain Metastases.

This new approach to avoiding this early detection of metastases is good for patients to reduce the mortality rate. Brain metastasis detection presents an opportunity for computer-aided detection (CAD), such as deep-learning-based approaches, due to the difficulty of the task and the serious consequences of missing a metastasis for patients, healthcare professionals, and the healthcare system. Fuzzy Genetic Algorithm and Artificial neural networks (ANN) and their variants, which are deep learning techniques, have been used more and more in data science classification and detection. Clinical issues have been addressed using ANN-related techniques. The genetic algorithm method has been used to analyze brain tumor datasets. The proposed approaches entail separating the best features and comparing the classification results with those of other approaches that have been described in the literature. A set of rules is applied to each axis used in the Artificial Neural Network classifications to adjust the fuzzy membership function and demonstrate the performance analysis with the classifications. The reason for this is that aggressive local development and metastasis occur frequently in metastases. It is estimated that metastasis is to blame for 90% of cancer-related fatalities. The goal is to locate early and eradicate brain metastases.

2. RELATED WORK

Jafar Abdollahi [3]. The main contribution, ensemble training methodology-based another Ensemble technique is stack generalization that combines lower-level models with a higherlevel model to improve prediction accuracy, and genetic algorithms were utilized to accurately diagnose Brain Metastases which are the primary breast cancer, and predict diabetes. But accuracy is low.

S. Shen, et al [4]. One of the major contributions is a novel magnetic resonance imaging (MRI) based method for diagnosing brain tumors. At first, the MR images underwent preprocessing, which included standardization and augmentation. Second, the brain was segmented into distinct tissues using an updated fuzzy clustering technique. Finally, brain tumors were located using fuzzy logic-based genetic programming (GP) to find classification rules. The technique seems promising based on classification findings on a variety of MR images for various diseases but did not take time into account.

T.Chithambaram et al. [5]. The significant aim, of this input collection, is for the Genetic Algorithm (GA) to find the set of optimal features. Two hybrid machine-learning models are utilized for pattern recognition. The Support Vector Machine (SVM) has been used to determine the initial likelihood of classifying tumors. Also, Artificial Neural Networks are used for confirmation of accuracy. But noise reduction is not used.

As was previously mentioned, a fuzzy-based genetic algorithm (FGM) algorithm was used to classify a large amount of data to eliminate noisy data, improve accuracy, and shorten the processing time. The fuzzy set of the rule is used to find the membership function to distinguish between Brain Metastases (MET) and other types of cancer cells as well as to display a graphical representation of the patient's health issues. Artificial neural network (ANN) classifiers are then used to categorize the excised transitional cancer cells, and the classification accuracy is compared.

3. PROPOSED WORK

The experiments compare real-time brain tumor MRI machinelearning database datasets with those from the UCI repository. The subsequent procedures are used to improve accuracy, shorten the time needed for data analysis, and eliminate noise from the data. By computing their heterogeneity parameters can compare the structural differences between diagnosed Brain Metastases which are primary lung cancer (LC), and melanoma cancer (MC) using 3D texture analysis (TA). Phase 1: Fuzzy genetic algorithms are used to identify the feature from a large amount of data. The features are classified using a fuzzy rules-based genetic algorithm and the unnecessary features are removed. Phase 2: A classification method using artificial neural networks (ANNs) has been used to gauge the depth of various tumor types to locate brain cancer metastases (LCBM and MCBM). It is also used to reduce noise and prevent overlap. Lastly, has been used to compare the algorithms using identical datasets.

4. METHODOLOGY

The experiment's research objective is to improve a CAD interface system that will help in the classification of numerous brain tumors. Two types of datasets are used to show the comparative performance analysis; the first dataset a diverse sample of 142 clinical patient records kept in real-time is being used for the research. It typically includes primary brain tumors like Glioblastoma Multiforme (GBM), Astrocytoma (AS), pediatric tumors such as Medullobla stoma (MED), and Meningioma (MEN), as well as secondary tumors such as Metastatic (MET), all of which were discovered using magnetic resonance imaging (MR). On slices of contrastenhanced T1-weighted (CET1) datasets, brain lesions were manually marked with the 3D region of interest (ROIs), and from each region, local binary patterns (LBP) maps were produced. The second dataset collected from the UCI repository includes a co-occurrence matrix and histogram based on minimum, maximum, variance, mean, standard deviation, correlation, contrast, entropy, energy, and homogeneity. Sliced the weighted average in 3D.

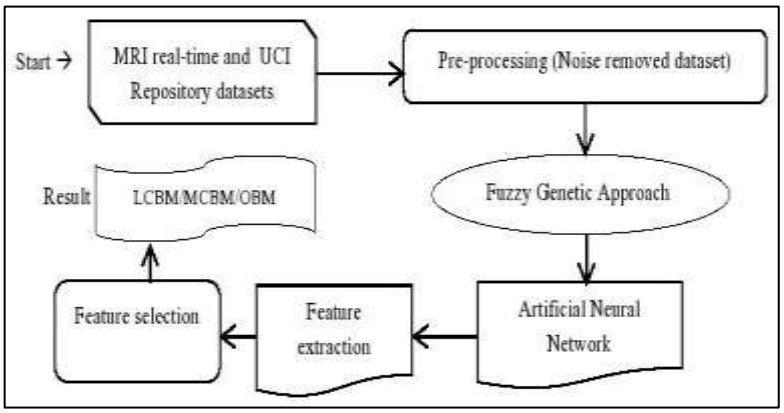

Figure 2. Early Detection Process of LCBM & MCBM

Fuzzy genetic algorithms and artificial neural networks (FGAANN) have been successfully used in the classification. The accuracy of prediction for various machine learning methodologies was evaluated using the proposed approach and compared with the aforementioned datasets; it scored 100% which, on the whole, outperforms earlier machine learning algorithms. In Fig 2, a knowledge representation technique is suitable for concepts. Fuzzy logic variables' truth value has

taken the range from 0 to 1, in contrast to traditional binary sets. The membership function serves as an extension of evaluation and represents the degree of truth. The concepts of natural selection and genetics are the foundation of the search-based optimization technique known as a genetic algorithm (GA). It has been used to locate ideal or nearly ideal answers to challenging issues that would otherwise take a lifetime to solve. It has been used to find true or approximate information to a problem involving optimization and search. Genetic algorithms are a class of global search heuristics. Concepts from evolutionary biology like inheritance, mutation, selection, and crossover are incorporated into this subclass of evolutionary algorithms. The new population is used in the iteration that comes after.
The study of healthcare and artificial intelligence (AI) is advancing quickly, with potential applications being shown in several medical specialities. The following processes are used to improve accuracy, shorten the processing time for data, and eliminate noise from the data. To increase the early detection of Lung and Melanoma Cancer metastases prediction performance or classification accuracy used by artificial neural network learning on purpose. When differentiating the Lung and Melanoma Cancers from the brain tumor dataset, in real-time datasets and UCI repository datasets are proposed fuzzy genetic and ANN approaches to produce higher classification accuracy than the current approaches, according to the results. Following these instructions have been shown how to find a crisp set using the fuzzy and categorization membership functions. 1. Fuzzy set of 2. Fuzzy genetic algorithm 3. Ambiguous genetic categories 4. Fuzzy Genetic membership function feature extraction.

4.1 Fuzzy Set

Numerous cancers have been identified using fuzzy logic a novel strategy. A fuzzy rule-based crisp set is the name given to the conventional bivalent set. The true/false presumption is the foundation of everything. There are two categories of items. They can be described as completely or partially contained inside a set. They are also referred to as Intersect and Union. A group of elements with continuous membership is referred to as a fuzzy set. Each object reflects the member's quality, which ranges from 0 to 1. This set is defined by the member properties' function. The content of this package includes notions like inclusion, union, intersection, complement, relatedness, and convexity [6]. After using two CSV files that represented sample data sets, the decision tables used the decision characteristics and condition attributes for fuzzy sets. The decision table is used to generate a clean set of intersects and unions.
The Hyperparameter is to be tuned. The datasets for machine learning on brain tumors are gathered here. The dataset is taken into account when testing each model. These datasets were obtained from the hospital in real-time and from UCI repositories for comparison to show the performance analysis. Using the same parameters as individual algorithms, we constructed various ANN frameworks to test whether fuzzy predictors created using genetic algorithm generalization increase the prediction accuracy for cancer metastases in the brain. Naturally, fuzzy logic has been chosen as the best feature to boost the suggested method's accuracy [7]. To preserve a portion of the original features, fuzzy reduces the number of attributes. Data preparation frequently employs feature selection to locate prior information.

4.2 Fuzzy genetic algorithm

John Holland proposed the first Genetic Algorithm (GA) in 1975. A genetic algorithm that makes use of fuzzy logic-based methods is called a fuzzy genetic algorithm (FGA). This blending aims to change the system parameters to increase the robustness and effectiveness of the performance in the genetic algorithms. Natural selection, the process that propels biological evolution, is used by the genetic algorithm to resolve constrained and unconstrained optimization problems. The genetic algorithm repeatedly modifies a population of unique solutions. In contrast to each data item only being a member of one, a data object in the fuzzy genetic algorithm (FGA) is a member of all data to varying degrees of fuzzy membership between 0 and 1 [8]. The objective of this unsupervised fuzzy classifier is to classify data into a predefined number of categories. Depending on how similar the data points are, each has a fuzzy membership to each group. Utilizing appealing learning and non-learning algorithms, initially divided the entity. The morphological filter has been linked to the removal of noise from data sets during filtering. A search engine that is based on genetic principles and natural selection is known as a genetic algorithm (GA). In a fuzzy system, GA is used to determine the membership functions and is prevalent in many scientific applications. The fuzzy system and genetic algorithm structure are as follows.

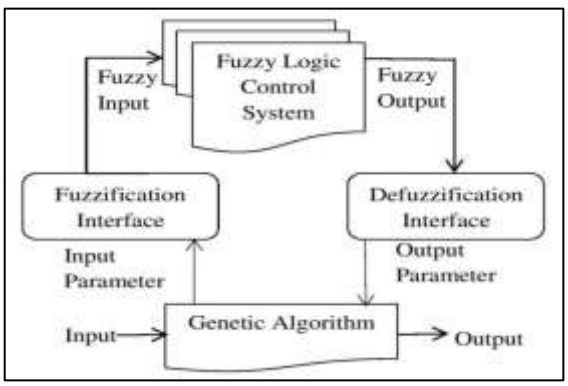

Figure 3. The FGA Structure

Using fuzzy genetics is a hybrid system. Fig 3, is designed to improve and model genetic algorithms using fuzzy logic-based techniques, and vice versa. A reliable and effective tool for completing tasks like creating the fuzzy rule base or the

membership function is the genetic algorithm [9]. In the FGA structure, input is first passed from the genetic algorithm, followed by input parameter passing to fuzzification, moving to the subsequent step of fuzzy logic, and finally getting the output. The following steps were used to do the genetic approach.

4.2.1 Genetic algorithm

GA is one of the earliest population-based random algorithms to have been proposed in human history. The most prevalent GA operations are select, cross, and mutant. These algorithms store important information in straightforward chromosomelike designs the structures that encode a potential answer to a particular problem using recombinant operators [10]. Although genetic algorithms come in a very wide variety, they are frequently thought of as performance optimizers.

4.2.2 Genetic Algorithm Parameters

In GA, additional parameters exist. It is necessary to change both structural and executive parameters, such as population size, and executive parameters like mutation and elite rates. However, this new approach used the most typical values for these variables, which produced pleasing outcomes, and the significance of the experiment's GA parameters. The GA method entails four crucial steps:

Chromosome1	11011 00100 110110
Chromosome2	10101 11000 011110
Offspring1	11011 11000 110110
Offspring2	10101 00100 011110

The characteristics were binary coded using genomes, with signifying selection and 0 signifying non-selection. Features that were eliminated are denoted by phenotypes with the label "0," while features that were chosen are denoted by phenotypes with the label "1". As a result, phenotypes with labels of 0 and 1 are referred to as decreased features and extremely significant features, respectively [11]. Each genotype then produces a group of subsets based on the idea of phenotypes. These subsets serve as training sets for the suggested method. The best features of each chromosome were then selected after being evaluated using the fitness function, and to produce a new generation of the population, the chromosomes underwent crossover and mutation. This process was repeated until the halting criteria were met. It was calculated how many people there were. The people who obtained the highest possible fitness scores were chosen using this ranking as a component of a selection strategy. A single-point crossover was then used to create the population [12].

4.2.3 Function of Fitness in GA

In this study, using a linear ranking value, the classifier's ability to fit the data was evaluated. The linear ranking is a statistical indicator of how closely expected and actual values match up. The training set's generation method affects the classifier's performance. Using a repeated sub-random sampling technique, cross-validation was carried out. The data were randomly split into training sets and testing sets before each GA analysis [13] & [14]. The linear ranking value allowed for the recording of each stage's performance. The linear ranking values centre was noted due to the significance of genome fit.

4.2.4 Crossover and Mutation

Crossover, also known as recombination, is a genetic operator used in genetic algorithms and combining the genetic info of two parents through evolutionary computation to create new offspring. In crossovers, two parents work together to care for the child. The process of selection (production) then comes to an end, and the appearance of higher individuals follows. In this study, a single-point crossover is used to pair two chromosomes. Slices from two chromosomes are taken once and switched between the two.

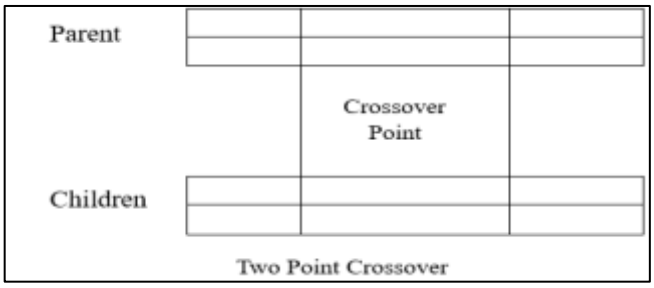

This is a particular application of the N-point Crossover method. The genetic material is exchanged at two randomly selected locations along the individual chromosomes (strings). After the crossing procedure is finished, the strings are added to carry out the mutation process. Small amounts are rotated from 0 to 1 and from 1 to 0 in touch mutations [15] &[16].

4.3 Fuzzy genetic classification

Brain tumor classification divides primary and secondary tumors into separate classes. Astrocytoma (AS), Glioblastoma Multiforme (GBM), Meningioma (MEN), Medulloblastoma (MED), and other primary brain tumors are examples. Cancer cells have spread to the brain in the form of secondary brain tumors or metastases (MET). The clinical patient records

(MRI brain tumors datasets) were collected from different excitation sequences, including T1, T2, and post-contrast T1. FLAIR offers details on the appearance and severity of brain tumors [17] & [18]. Brain tumors are more visible on post-contrast T1-weighted MRI datasets than on other sequences. The intravenous administration of 0.15-0.20 ml/kg of MR results in the postcontrast T1 images' dataset.

4.4 Feature extraction in the fuzzy genetic membership function

FGA can be used to compute membership functions in a fuzzy logic system, in addition to being used to find the best solution to a problem. A genetic algorithm that uses fuzzy logic is known as a fuzzy genetic algorithm (FGA). By changing the system parameters, this blending aims to improve the efficiency of the genetic algorithms. The brain is the site of about onefourth of all cancer metastases [19] & [20]. The main method for identifying Brain Metastases, planning radiotherapy, and keeping track of treatment effectiveness is magnetic resonance imaging (MRI). As these therapies are most effective when applied to small, subcentimeter-sized metastases, progress in tumor treatment now depends on their detection.

The GA operations to be determined Crossovers, which produce a new chromosome from two parents, are a fundamental characteristic of GAs. Crossovers are the exchange of individual information. After being chosen based on their fitness values and gathered into a gene pool, individuals are crossed over. Three stages of crossover take place. The initial phase is matching. The random selection of two people from a gene pool is known as matching. Finding a crossover point in each of the individuals is the second stage. In the final phase, two people are swapped out for one another [21] & [22]. A mutation is an arbitrary change in a chromosome's information that takes place for no discernible reason. In other words, chromosome variation is determined by a process called a mutation. This variation might be regional or worldwide. It is decided whether a mutation will be applied based on a probability test. For instance, if the average fitness of the new generation is lower than the average fitness of the previous generation, but y of chromosome x can be changed.

Using the prototype and the idea of a fuzzifier m being used to determine the membership value of data X_k, one can ascertain the value measure of a member of a given dataset. When k = 1, 2...n and I = 1, 2...c are employed to represent the membership and value of X_k, respectively, a genetic accurately reflects these variables. For GA, it is essential to comprehend the initial desired point. The membership value is the distance from the centre of the point V_i to the set X_k. FGA expands the scalar membership to a triangular secondary membership function when restricting the triangular and trapezoid membership function for a fuzzy set. The genetic algorithm is expressed verbally as a sequence of uncertain upper and lower numbers. The linguistic ambiguity value is specified using the fuzzy set of m [23] & [24]. The fuzzy genetic algorithm's fuzzifier value has been expressed using two linguistic representations of the fuzzifier m that make use of fuzzy sets. FGA: the vertical slice of x, and the membership value for x in the sample.

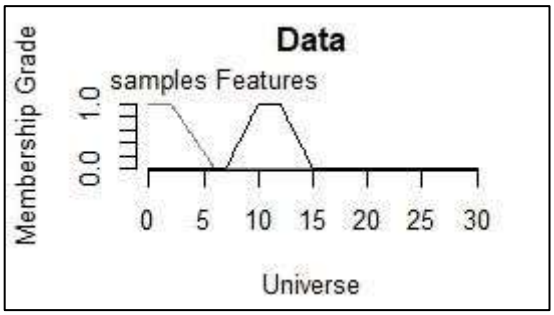

Figure 4. Universe of sample datasets

The membership function is added using Fig. 4, which also specifies the universe of sample datasets made up of features and sets the universe's options sequentially from 0 to 30 by 5. The membership grade ranged from 0.0 to 1.0 and was worth 0.2 points.

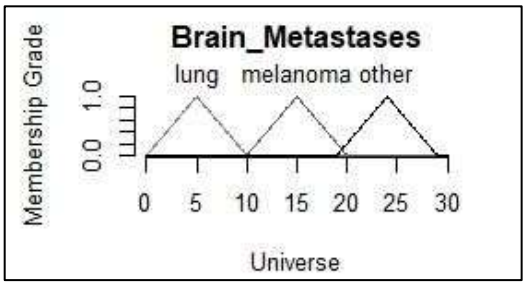

Figure 5. Triangular Membership Function

The mathematical simplicity of the triangular membership functions feature, which is used in Fig 5, is notable. It is specified by the three parameters lung, melanoma, and other cancer metastases, and the membership function Fig 5 depicts the fuzzy trapezoid partition function's LC and MC from the Brain Metastases fuzzy partition variables. These fuzzy partition variable names are lung = 0-10, melanoma = 10-20, other = 20-30, sd = 1.5, and fuzzy cone radius = 5.

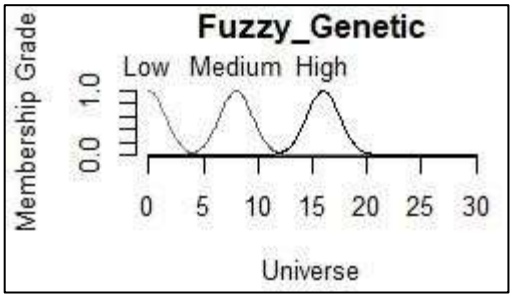

Figure 6. Trapezoid Membership Function

In Fig 6, the trapezoid Membership Function uses fuzzy partition gene rules and illustrates fuzzy partition variables. The Trapezoidal Rule divides the total area into smaller trapezoids rather than using rectangles to calculate the area under the curves. This integration calculates the area by approximating the region underneath a function's graph as a trapezoid. The fuzzy trapezoid membership function is composed of metastatic cancers, including lung cancer (LC), Melanoma Cancer (MC), and unknown cancer (UC). The applied fuzzy partition variable names—LC= 0, MC= 5, UC= 12, and fuzzy cone radius= 5—illustrate the application of three fuzzy rules to a trapezoid formed by low, medium, and high. To extract the specific and produce the data, three rules are applied; each rule has been given in a fuzzy partition based on fuzzy logic [25]. Following TA, four separate extractions and calculations of subset textures were made. The operating characteristic analysis was used to examine each texture's ability to categorize the various lung carcinoma and melanoma types. To create models and enhance TA's predictive power, the fuzzy genetic algorithm and artificial neural network-based feedforward propagation classifier models were used.

5 DETECTION OF LUNG AND MELANOMA CANCER IN BRAIN METASTASES BASED ON ARTIFICIAL NEURAL NETWORKS (ANN)

About one-fourth of all cancer metastases are found in the brain. Magnetic resonance imaging(MRI) is the primary method for identifying Brain Metastases, organizing radiotherapy, and gauging treatment effectiveness. At the subcentimeter level, where these drugs are most potent, it is now necessary to detect new or developing metastases to advance tumor treatment [26]. Artificial neural networks were developed in part as a result of the complex neuron system's processing of data and information for learning and knowledge establishment. Differentiating melanoma from various lung and brain metastases, and other cancers required highly precise texture data-based lesion classification. In terms of prediction, the combined FGA and ANN-based back propagation model performed better than the earlier model. Using the Brain Metastases datasets, the new method has successfully identified lung and melanoma metastases [28].

5.1 Artificial Neural Network (ANN)

The objective is to develop an MRI-based deep-learning method to detect Brain Metastases. The axial post-contrast 3D T1-weighted imaging sequence, the 1.5T and 3T field strengths, and the total population of the scans The faster region-based artificial neural network was trained and tested using data from 142 patients' clinical datasets. The study type is retrospective [29]. MRI is widely used in the prognosis of brain metastases from lung and melanoma cancer. One possible way to get around this restriction is to use texture analysis (TA) on the MRI data textures are complicated network patter nation patterns that can be identified by their brightness, color, slope, and size. Texture carries a lot of information about how a physical structure was constructed and can be used to interpret and analyze datasets [30].

Although a computer might have trouble deciphering the texture, humans can easily recognize it. The complex patterns have been mathematically quantified and these texture components have been interpreted using TA. Several factors that are thought to influence the performance of lung and melanoma metastases were outlined after a thorough review of the literature and consultation with Brain Metastases. Within the framework of the ANN modeling, these variables were carefully considered and synchronized into a manageable number suitable for computer coding. These variables were categorized as inputs. Whether the patient has lung, melanoma, or other cancer metastases, the output variables represent some likely levels of performance for Brain Metastases. The TA was also performed on the images from the other three series T1weighted series, T2-weighted series, and diffusion of the weighted imaging clinical dataset series. A propagation ANN classifier approach was used to enhance classifier accuracy [31]. A type of artificial intelligence known as artificial neural networks (ANNs) has the benefits of adaptability, parallel processing, and non-linear processing. They are frequently employed in the diagnosis and detection of tumors. In this article, we'll talk about how ANNs were created, how they work, what they look like, and how much research is currently being done on using them to find and diagnose Brain Metastases [32].

A computational model with biological roots known as an artificial neural network consists of thousands of artificial neurons connected by coefficients and weights to simulate the neural architecture. Because they process information, they are referred to as processing elements (PE). A transfer function, weighted inputs, and a single output are all features of each PE. In its simplest form, PE is an equation that balances inputs and outputs. As a result of the connection weights representing the system's memory, ANNs are also referred to as connectionist models. Even though a single neuron is capable of performing specific, straightforward information processing tasks, the strength of neurons in a network is connected to produce neural computations. There are valid arguments for and against the alleged intelligence of artificial neural networks. Contrary to artificial neural networks, which rarely have more than a few hundred or thousand PEs, the human brain has 100 billion neurons. The different kinds of neural networks that have been developed to date have all

been categorised using the transfer functions of the neurons, the connection formula, and the learning rule. Weekly, new ones are created [33].

5.2 Artificial Neurons

The artificial neuron is part of an ANN whose structure is intended to mimic a biological neuron's functionality. The output for that neuron is created by multiplying the connection weights (adjusted), which are completed first, by the incoming signals, also referred to as the inputs. The activation function is the weighted sum of the inputs to the neuron, and the most popular transfer function is the sigmoid function.

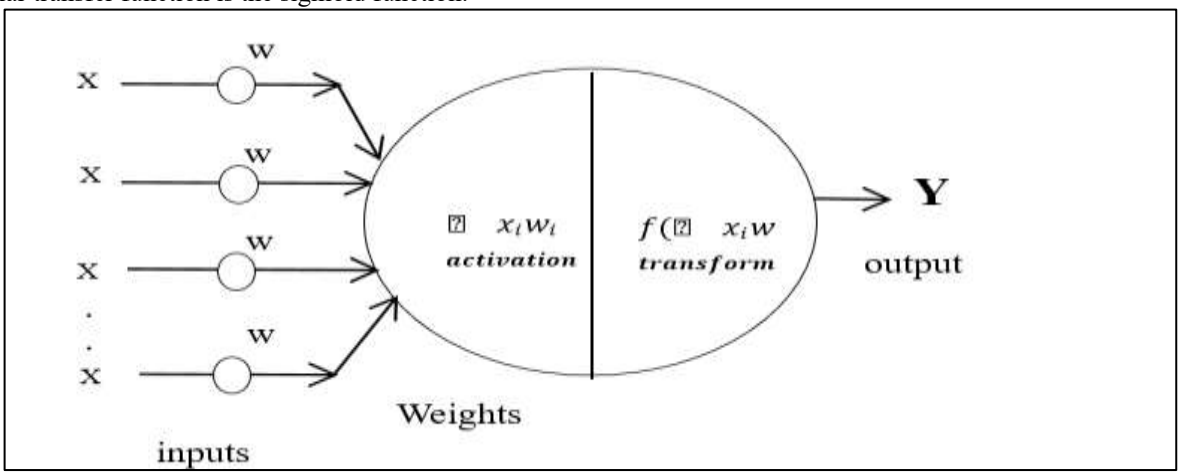

Figure 7. Sigmoid Function

In Figure 7, where x1, x2 and x3 are inputs, w1, w2 and w3 weights, $\sum x_i w_i$ is the activation function, $f(\sum x_i w_i)$ is the transform, and y is the output. Before the final prediction of a class score for each label in a linear model, the hidden layers perform the linear mapping of an input function to an output [34]. The input layer receives data in various formats, such as images, videos, texts, speech, sounds, or numeric data, and transforms them into vectors x, whose transformation is defined by

$$f(x)w^{T}x + b \quad (1)$$

here w = weights, b = biases, and x = input. To comprehend the data's patterns, The mappings from equ.1 also yield linear results from the neural networks, and the Activation Functions (AF) change these linear results into non-linear results for additional propagation. The results are attained through

$$y = (w_1 x_1 + w_2 x_2 + \cdots w_n x_n + b) \quad (2)$$

For multi-layered networks like ANN, the layer receives these outputs below it until the desired result is obtained. However, the kind of AF to deploy in a specific network depends on the expected results. While the outputs are linear, a nonlinear AF is required to convert them to nonlinear outputs. After the AF is applied, the nonlinear output is given by

$$y = \alpha(w_1 x_1 + w_2 x_2 + \cdots w_n x_n + b) \quad (3)$$

Where the activation functions (AF) are for deeper networks, the AF facilitates the learning of higher-order polynomials in the network structure whose positions depend on their functions. In addition, we are interested in comprehending the composition of the various layers, with a focus on the AFs.

5.3 Connection of formula

The method used to connect the neurons significantly affects how the artificial neural network functions. Inputs that are both excitatory and inhibitory can reach artificial neurons, just like real neurons. The next neuron's summing mechanism adds in response to excitatory inputs while subtracting in response to inhibitory inputs. In the same layer, a neuron has the power to stop other neurons from acting. The term for this is lateral inhibition [35]. The network's objective is to choose the most likely candidate and suppress all others. Competition is another name for this idea. Another type of connection is feedback, in which the output of one layer is returned to the input of a succeeding layer or the same layer. Depending on whether a network has feedback connections or not, Two types of architecture have been identified. A feedforward architecture's output does not connect back to the input neurons, so it does not remember its previous output values.

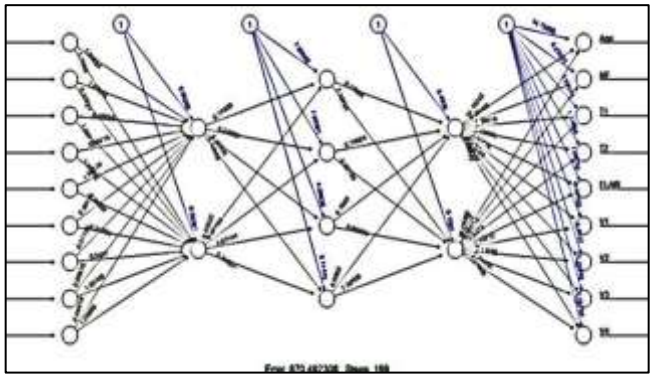

Figure 8. ANN Real-time architecture with hidden layers

Therefore artificial neural network uses back-propagation in Figure 8. The qualities Age, Sex, T1, T2, FLAIR, V1, V2, V3, and V4 make up the propagation. Both neurons are coupled for forwarding and backward propagation in the illustration. In Fig 8, all of the layers carry error signals. Through 189 steps, 870.492308 error rates are calculated. Backpropagation involves calculating an error signal by contrasting the network's output with the desired output. The ensuing erroneous signal travels layer by layer backwards through the network. The forward network's weight connections are updated in this study using the stochastic gradient descent back propagation method. When the forward propagation parameters are altered, the error signal is sent back to the layer and subsampling layer. The subsampling layer multiplies the local gradient.

Where Fig 9. The data collected from UCI included 1801 MRI datasets and the features are mean, variance, standard deviation, entropy, skewness, kurtosis, contrast, energy, ASM, homogeneity, dissimilarity, correlation, coarseness, class and the neurons make up the hidden layer that determines the weight value. All the layers carry error signals, through 115 steps, 869.107694 error rates are calculated. The weight value serves as the processing capacity's measure of the inter-unit connection strength. Last but not least, bias is another name for the blue number. Neurons in the feedback architecture are connected from the output to the input.

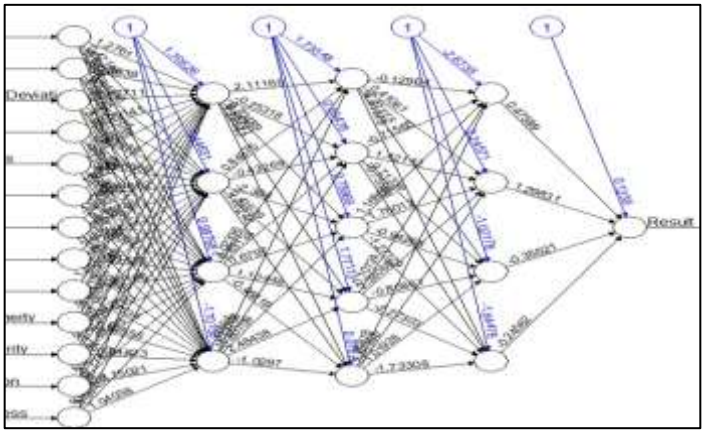

Figure 9. ANN UCI repository architecture

When attempting to reduce the training error, each neuron has an additional input weight of one, allowing for an additional degree of freedom. Such a network keeps track of previous states so that the current state is influenced by both input signals and previous network states.

5.4 Learning of neurons rule

Although there are many diverse learning of neuron rules, the Delta rule or Back-propagation rule is the one that is most frequently applied. By the number of iterations adjusting the weights, a neural network has been trained to map a set of input data [36]. The use of weighted links has a significant impact on the ANN's recognition ability. The network improves the weights between neurons by using information from inputs. In the training or learning phase, the weights are optimized by backward propagation of the error. To reduce the discrepancy between the predicted and target values, the ANN reads the input and output values from the training data set and modifies the value of the weighted links. The prediction error is decreased over numerous training cycles until the network reaches the desired level of accuracy [38].

5.5 Extraction of Texture Features and Pathological Classification

It was crucial to identify texture characteristics that remained constant across measurements. At first, the extracted texture features had to be incredibly repeatable. The concordance correlation coefficient in this study could ensure reproducibility if the CCC is 0.9. The capacity to choose high levels of differentiation in features was also crucial. To accomplish this, we used the dynamic range (DR) metric. Similar to CCC, DR _0.9 denoted a wide dynamic range for the feature [39] & [40]. When I select a particular sample from the n-patient cases, the maximum and minimum are computed on the entire sample

set. The DR has a range of 0 to 1. To further improve the discriminative power and minimize the feature vector's size, fuzzy analysis, and genetic algorithm analysis were applied. Because all observations were used for both training and validation, the method had an advantage over repeated random subsampling, which increased the fuzzy genetic and ANN classifier reliability of the models [41 - 45]. To increase classifier accuracy, the propagation artificial neural network classifier model was used. The perfect prediction represented by an ANN value of +1, no better than random prediction by 0, and completes disagreement between prediction and observation by -1.

6 RESULTS AND DISCUSSION

The noisy data cannot be handled by fuzzy genetic techniques alone. Fuzzy genetics applied in the membership function with an integrated ANN. The table below provides a summary of the sample dataset used to reduce noise, improve accuracy, and speed up processing.

Table 1. The real-time brain tumors dataset MRI machine learning database

Age	MF	T1	T2	FLAIR	V1	V2	V3	V4
30	F	0	0	0	0	0	1	1
40	F	2.7	2.7	2.5	0	0	0	1
50	F	4.7	4.5	3.5	0	0	0	4
60	M	6.5	5.4	5	0	0	1	1
35	M	4.3	3.7	3.4	0	0	0	1
30	F	3.9	3.7	3.7	0	0	0	1
42	F	0	0	0	0	0	1	1
42	F	5	4.6	4.5	0	0	1	1

Table 1 shows each data set including the number of features (real-time dataset attributes). To illustrate the prediction value, the fitted value between 0 and 1, is also referred to as the predicted value 0, 1, or near 1. With this prediction, the value was found accurate.

Table 2. The MRI brain tumors dataset machine learning database from UCI

Mean	Variance	Standard Deviation	Entropy	Skewness	Kurtosis	Contrast	Energy	ASM	Homo Geneity	Dis Similarity	Correlation	Coarseness
6.111084	243.7205	15.61155	0.103618	2.954798	9.017418	56.96668	0.284868	0.08115	0.571593	2.995662	0.949621348	7.46E-155
5.288712	247.9202	15.74548	0.176847	3.422888	12.19064	52.30651	0.379754	0.144213	0.633933	2.644769	0.96687865	7.46E-155
9.117813	392.482	19.81116	0.128204	2.762934	8.889926	77.18562	0.319556	0.102116	0.580501	3.230422	0.952995025	7.46E-155
4.900024	208.1788	14.4284	0.113485	3.332554	11.40327	54.2702	0.298902	0.089342	0.590712	2.849782	0.954351982	7.46E-155
8.348267	783.3388	27.98819	0.167314	3.711011	14.10537	156.2022	0.368764	0.135987	0.61127	3.781917	0.972981116	7.46E-155
14.63995	1193.582	34.54826	0.131848	2.741492	7.791452	200.2366	0.324392	0.10523	0.581015	4.513547	0.962503485	7.46E-155
10.57385	1478.247	38.44798	0.016741	4.023409	16.57684	180.7677	0.110225	0.012149	0.414323	4.949008	0.972513378	7.46E-155
9.267914	1269.065	35.62394	0.013323	4.224468	18.33831	140.571	0.098035	0.009611	0.392873	4.783454	0.973460268	7.46E-155
2.416336	317.8541	17.82846	0.039081	7.665443	59.94971	435.9922	0.170671	0.029128	0.449634	6.896724	0.925062675	7.46E-155
19.79886	1512.742	38.89399	0.096563	2.359342	5.821872	151.7432	0.27463	0.075421	0.562647	4.104189	0.970727005	7.46E-155
15.73924	1572.819	39.65878	0.004629	3.011192	9.480986	145.6549	0.056951	0.003243	0.385197	4.944483	0.94087978	7.46E-155

In Table 2, each data collection included a sample of the classes, features, and attributes; only a handful of the features from the datasets are displayed in the table.

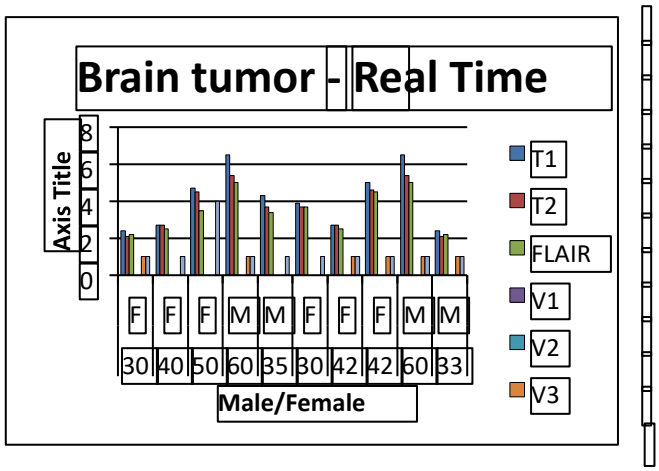

Figure 10. The real-time dataset histogram

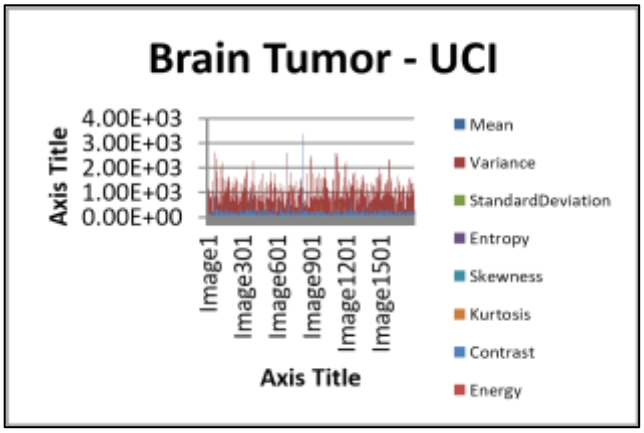

Figure 11. UCI repository dataset histogram

The performances of the real-time dataset's histogram are compared in Fig. 10. Similarly, the performances of the UCI repository dataset's histogram are compared in Fig. 11.

Table 3. Real-time Datasets Classification Accuracy Results

FGA	FGA-RED	FGA-ANN	FGA-RED-ANN
91.65%	92.55%	96.67%	97.66%

Finally, table 3 has the overall performance of real-time datasets to show the Fuzzy Genetic Algorithm (FGA) and artificial Neural Networks (ANNs) based reduction (RED). The table portrays the accuracy attained by the FGA, FGA-RED, FGA-ANN and FGA-RED-ANN accuracy are, 91.65%, 92.55%, 96.67% and 97.66%. Showing the fuzzy genetic reduction integrated with the ANN result is the highest value at 97.66%.

Table 4. UCI repository datasets Classification Accuracy Results

FGA	FGA-RED	FGA-ANN	FGA-RED-ANN
93.65%	94.55%	98.16%	100%

The overall performance of UCI datasets showed the FGA and ANN in Table 4. The percentages are as follows: FGA 93.65%, FGA-RED 94.65%, FGA-ANN 98.16%, and FGARED-ANN 100%, according to the table. The highest result, 100%, is displayed by FGA-RED-ANN.

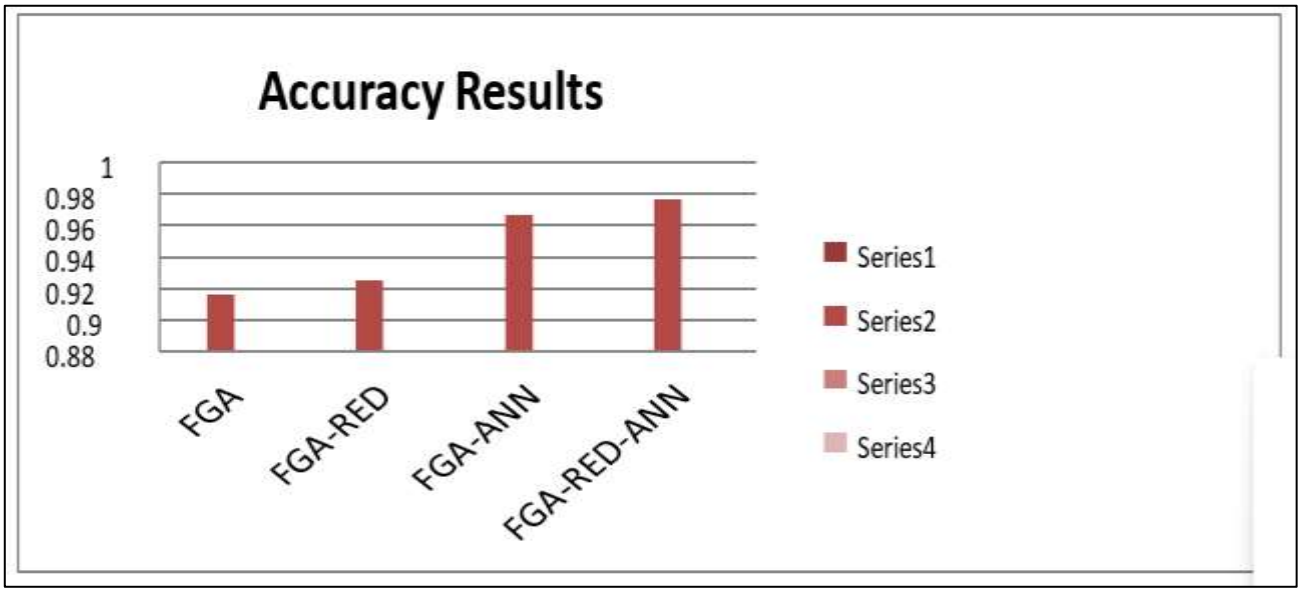

Figure 12. Real-time dataset classification accuracy results

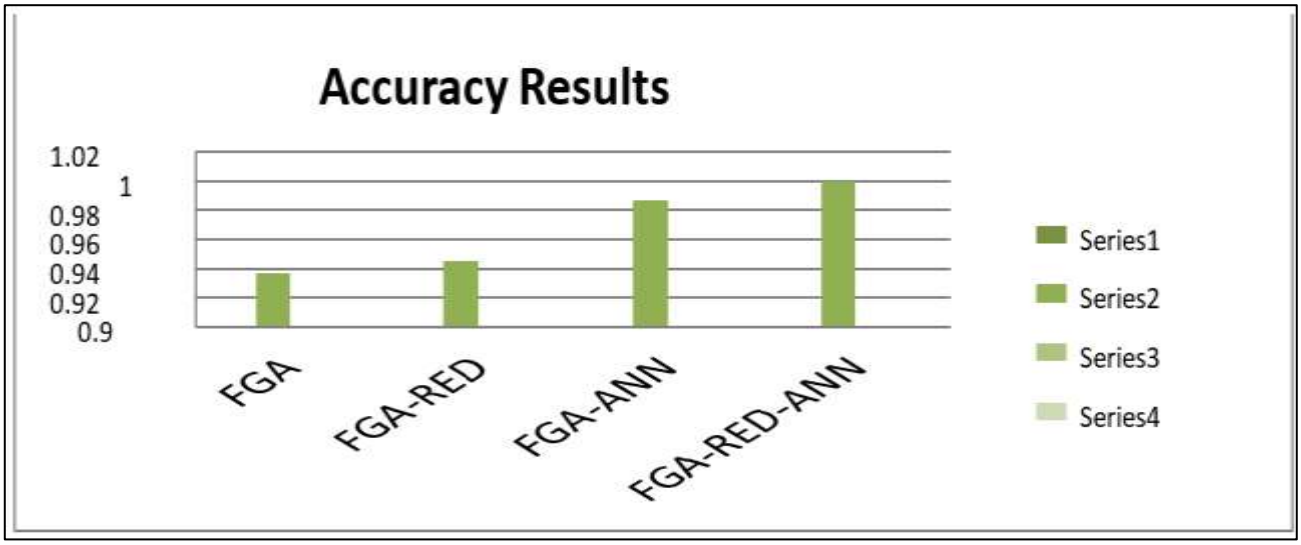

Figure 13. UCI repository datasets Classification accuracy results

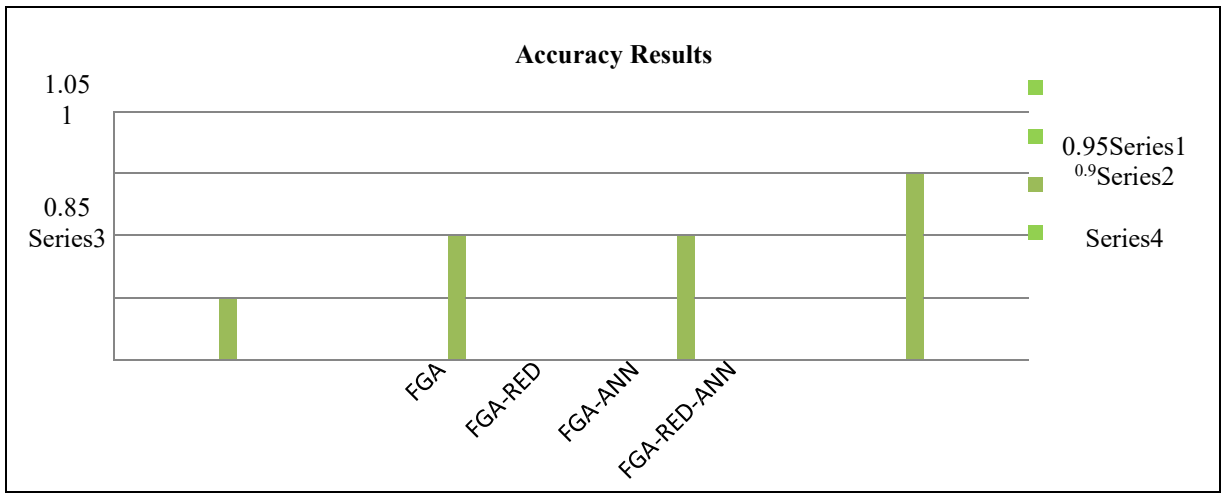

Figure 14. Brain tumor classification accuracy using real-time datasets and UCI repository datasets

7. CONCLUSION

TA has predicted the differences between various pathological types of lung and melanoma cancer metastases in the brain. The texture parameters, which represent the tumor histopathology structure and may be used as an additional diagnostic tool, require more study. Tools for soft computing were taken into consideration to investigate a new approach. Comparing and analyzing the training and test datasets. Test data had the highest prediction value when compared to the other two, it was discovered. The problem of how to extract lung and melanoma from the Brain Metastases, from MRI sample data, was systems studied using FGA and FGA-ANN. The ambiguous membership function has been linked with the FGA and ANN to create useful value-added approaches to handle uncertainty. Consequently, categories for making decisions result in a useful tool. Cross-validation has been used with ANN to get good classification performance for sizable datasets. The output of the artificial neural network data extraction reveals the prediction value. Consequently, categories for making decisions result in a useful tool. The dataset for the FGA and ANN model data that extracts the MRI output displays the prediction value. Additionally, the accuracy of FGA-REDANN is higher than other solutions with scores from realtime datasets 91.65%, 92.55%, 96.67%, 97.66%, and from UCI repository datasets 93.65%, 94.65%, 98.16%, 100%, for FGA, FGA-RED, FGA-ANN, and FGA-RED-ANN. Respectively FGA-RED-ANN is effectively dealing with the early detection and prevention of lung and melanoma metastases.

REFERENCES

1. F. Bertolini, A. Spallanzani, A. Fontana, R. Depenni and G. Luppi, “Brain Metastases: an overview,” CNS Oncology., vol. 4, no. 1, pp.37–46, Jan. 2015.
2. K. H. Chen, K. J. Wang, A. M. Adrian, K. M. Wang and N. C. Teng, “Diagnosis of Brain Metastases from lung cancer using a modified electromagnetism like mechanism algorithm,” Journal of Medical Systems., vol. 40, pp. 1-14, Jan. 2016.
3. J. Abdollahi and B. Nouri-Moghaddam, “Hybrid stacked ensemble combined with genetic algorithms for diabetes prediction,” Iran Journal of Computer Science., vol.5, no. 3, pp. 205–220, Sep. 2022.
4. S. Shen, W. A. Sandham, M. H. Granat, M. F. Dempsey and J. Patterson, “A New Approach to Brain Tumour Diagnosis using Fuzzy Logic Based Genetic Programming,” IEEE Engineering in Medicine and Biology., vol. 1, pp. 870–873, Sep. 2003.

5. T. Chithambaram and K. Perumal, “Brain Tumor Segmentation using Genetic Algorithm and ANN Techniques,” Power, Control, Signals and Instrumentation Engineering., pp. 970–982, Sep. 2017.
6. Jeyavani M. and Karuppasamy M., EEG in Optic Nerves Disorder Based on FSVM Using Kernel Membership Function. Springer. Vol. 1, pp. 145154, Oct. 2022.
7. M. Kissi, M. Ramdani, M. Tollabi and D. Zakarya, “Determination of fuzzy logic membership functions using genetic algorithms: application to structure–odor modeling,” Journal of molecular modelling., vol. 10, pp. 335-341, 2004.
8. A. K. Anaraki, M. Ayati and F. Kazemi, “Magnetic resonance imaging-based brain tumor grades classification and grading via convolutional neural networks and genetic algorithms,” biocybernetics and biomedical engineering., vol. 39, no. 1, pp. 63-74, Jan 2019.
9. M. Jansi Rani and D. Devaraj, “Two-Stage Hybrid Gene Selection Using Mutual Information and Genetic Algorithm for Cancer Data Classification,” “Journal of Medical Systems.” Vol. 43, pp. 1-11, Aug. 2019.
10. M. Jansi Rani and D. Devaraj, “Microarray Data Classification using Multi Objective Genetic Algorithm and SVM, ” Intelligent Techniques in Control, Optimization and Signal Processing., pp. 1-3, Apr. 2019.
11. Xiang Li, Qiao Chen, and Yanli Li, “Impact on Genetic Algorithm of Different Parameters,” Computation and Intelligence., pp. 479–488, Dec. 2008.
12. S. Oh, J. Yoon, Y. Choi, Y. A. Jung and J. Kim, “Genetic Algorithm for the Optimization of a Building Power Consumption Prediction Model.” Electronics, vol. 11, no. 21, 3591, Nov. 2022.
13. LS Shafti, E Pérez, “Fitness Function Comparison for GA-Based Feature Construction,” Artificial Intelligence., vol. 12, pp. 249–258, Nov. 2007.
14. M. Jansi Rani and M. Karuppasamy, “Cloud Computing-Based Parallel Mutual Information For Gene Selection And Support Vector Machine Classification For Brain Tumor Microarray Data”, NeuroQuantology., vol. 20, no. 6, 6223-6233, 2022.
15. M. Arif, F. Ajesh, S. Shamsudheen, O. Geman, D. Izdrui and D. Vicoveanu, “Brain tumor detection and classification by MRI using biologically inspired orthogonal wavelet transform and deep learning techniques,” Journal of Healthcare Engineering., 2022.
16. M. Jansi Rani and D. Devaraj, “Two Stage Hybrid Gene Selection using Mutual. Information and Genetic Algorithm for Cancer Data Classification,” Journal of Medical System., vol. 43, pp. 1 – 11, 2019.
17. K. Takano, M. Kinoshita, M. Takagaki, M. Sakai, S. Tateishi, T. Achiha, R. Hirayama, K. Nishino, J. Uchida, T. Kumagai and J. Okami, “Different spatial distributions of brain metastases from lung cancer by histological subtype and mutation status of epidermal growth factor receptor,” Neuro-oncology., vol. 18, no. 5, pp. 716-724, May 2016.
18. M. Jansi Rani and D. Devaraj, “Multi-class cancer classification in microarray datasets using MI-based feature selection and artificial neural network,” Nanoelectronics, Circuits and Communication Systems, pp. 107-115, 2018,
19. A. Averkin and S. Yarushev, “Fuzzy Approach to Explainable Artificial Intelligence,” Theory and Applications of Fuzzy Systems and Soft Computing., pp. 180-187, Aug. 2022.
20. M. Jansi Rani, M. Karuppasamy and M. Prabha, “Bacterial foraging optimization algorithm based feature selection for microarray data classification,” Materials Today: Proceedings., Jan. 2021.
21. FJ. Pinto, “Operation of a Genetic Algorithm Using an Adjustment Function,” Distributed Computing and Artificial Intelligence., pp. 21-30, Jul.2023.
22. M. Jansi Rani and D. Devaraj, “A Combined Clustering and Ranking based Gene Selection for Microarray Data Classification,” Computational Intelligence and Computing Research., pp. 1-5, 2017.
23. J. Sachdeva, V. Kumar and I. Gupta, “Multiclass Brain Tumor Classification using GA-SVM,” Developments in E-systems Engineering., pp. 182187, Dec. 2011.
24. M. Jansi Rani and D. Devaraj, “Microarray Data Classification using Multi Objective Genetic Algorithm and SVM,” Intelligent Techniques in Control, Optimization and Signal Processing., pp. 1-3, Apr. 2019.
25. D.R. Lakshmi and S.S. Begum, “An Optimization Technique for Brain Tumour Recognition,” International Journal of Computer Science and Information Security., vol. 14, no. 6, Jun. 2016.
26. V. Rezaie and A. Parnianifard, “A new intelligent system for diagnosing tumors with MR images using type-2 fuzzy neural network,” Multimedia Tools and Applications., pp. 1-31, Jan. 2022.
27. R.Y. Fan, J.Q. Wu, Y.Y. Liu, X.Y. S.T. Liu, Qian, C.Y. Li, P. Wei, Z. Song and M.F. He, “Zebrafish xenograft model for studying mechanism and treatment of non-small cell lung cancer brain metastasis,” Journal of Experimental & Clinical Cancer Research., vol. 40, pp.1-15, Dec. 2021.
28. A. O. Levey, M. Elsayed, D. H. Lawson, R. M. Ermentrout, R. R. Kudchadkar, Z. L. Bercu, M. L. Yushak, J. Newsome and N. Kokabi, “Predictors of Overall and Progression-Free Survival in Patients with Ocular Melanoma Metastatic to the Liver Undergoing Y90 Radioembolization,” CardioVascular and Interventional Radiology., vol. 43, pp. 254–263.Feb, 2020.
29. M. Sharma, G. N. Purohit and S. Mukherjee, “Information Retrieves from Brain MRI Images for Tumor Detection Using Hybrid Technique K-means and Artificial Neural Network,” vol.2, pp. 145-157, 2018
30. S. Abu Naser, I. Zaqout, M. A. Ghosh, R. Atallah and E. Alajrami, “Predicting Student Performance Using Artificial Neural Network,” Faculty of Engineering and Information Technology., vol. 8, no. 2, pp. 221-228, 2015
31. A. Elzamly, B. Hussin, S. S. Abu Naser, T. Shibutani and M. Doheir, “Predicting Critical Cloud Computing Security Issues using Artificial Neural Network (ANNs) Algorithms in Banking Organizations,” Faculty of Engineering and Information Technology., vol. 6, no.2, pp. 40-45, Apr. 2017.

32. R. Ortiz-ramón, A. Larroza, S. Ruiz-españa, E. Arana and D. Moratal, “Classifying Brain Metastases by their primary site of origin using a radiomics approach based on texture analysis : a feasibility study,” European radiology., vol. 28, pp. 4514-4523, Nov. 2018.
33. D. Bhattacharyya and T. Kim, “Brain Tumor Detection Using MRI Image Analysis,” Ubiquitous Computing and Multimedia Applications., pp. 307–314. Apr. 2011
34. D. Wajeeh, A. Kashf, A. N. Okasha, N. A. Sahyoun, R. E. El-rabi and S. S. Abu-naser, “Predicting DNA Lung Cancer using Artificial Neural Network,”International Journal of Academic Pedagogical Research., vol. 2, no. 10, pp. 6–13, Oct. 2018.
35. S. Owen and L. Souhami, “The management of Brain Metastases in non-small cell lung cancer,” Frontiers in Oncology., vol. 4, pp. 1–6, Sep. 2014.
36. C. Nwankpa, W. Ijomah, A. Gachagan and S. Marshall, “Activation Functions: Comparison of trends in Practice and Research for Deep Learning,” 2018.
37. Z. Li, Y. Mao, H. Li, G. Yu, H.Wan and B. Li, “Differentiating Brain Metastases from different pathological types of lung cancers using texture analysis of T1 postcontrast MR,” Magnetic Resonance in Medicine., vol. 76, no. 5, pp. 1410–1419, Nov. 2016.
38. H. Shen, G. Deng, Q. Chen and J. Qian, “The incidence, risk factors and predictive nomograms for early death of lung cancer with synchronous brain metastasis: a retrospective study in the SEER database,” BMC Cancer., vol. 21, no. 1, pp.1–17, Dec. 2021.
39. W. Schuette, “Treatment of Brain Metastases from lung cancer: Chemotherapy,” Lung Cancer., vol. 45, pp. S253-S257, Aug. 2004.
40. Menu, A., Targets, C., & Aspects, C. (1996). Share Announcement Question _ Answer Question _ Answer Thumb _ Up Textsms. 6, 1–4.
41. G. Toyokawa, T. Seto, M. Takenoyama and Y. Ichinose, “Insights into brain metastasis in patients with ALK+ lung cancer: is the brain truly a sanctuary?,” Cancer and Metastasis Reviews., vol. 34, pp. 797–805, Dec. 2015.
42. K. Michael Mahesh and J. Arokia Renjit, “Evolutionary intelligence for brain tumor recognition from MRI images: a critical study and review,” Evolutionary Intelligence., vol. 11, no. 1–2, pp. 19–30, Oct. 2018.
43. L. Nayak, E. Q. Lee and P. Y. Wen, “Epidemiology of Brain Metastases,” Current Oncology Reports., vol. 14(1), pp. 48–54, Feb. 2012.
44. M. Elhoseny, G.B. Bian, S.K. Lakshmanaprabu, K. Shankar, A.K. Singh and W. Wu, “Effective features to classify ovarian cancer data in internet of medical things,” Computer Networks, 159, pp.147-156, Aug. 2019.
45. M. Jansi Rani and D. Devaraj, “Multi-class Cancer Classification in Microarray Datasets using MI-based feature selection and Artificial Neural Network,” Nano-electronics, Circuits & Communication Systems, pp. 107-115, 2020.